Acta Crystallographica Section A
Foundations of Crystallography
ISSN 0108-7673

Received 23 February 2000
Accepted 31 October 2000

Statistical dynamical direct methods. II. The three-phase structure invariant

F. N. Chukhovskii, J. J. Hu and L. D. Marks*

Department of Materials Science and Engineering, Northwestern University, Evanston, IL 60208-3108, USA. Correspondence e-mail: l-marks@nwu.edu

The triplet distribution used for kinematical diffraction is extended to the complex case appropriate for dynamical transmission electron diffraction. It is demonstrated that this gives good results if the distributions are handled statistically rather than relying upon single triplet relationships. As a consequence, conventional statistical direct methods will yield a reasonable approximation to the effective dynamical potential for thicknesses when kinematical theory is not appropriate. The recovered effective dynamical potential may be similar to the kinematical potential, but does not have to be and in general will not be.

1. Introduction

A classic problem in transmission electron diffraction (TED) and microscopy is to determine at least approximately the atomic structure. Over the last 15 years, there has been substantial success using high-resolution electron-microscopy (HREM) techniques, coupled appropriately with image simulations and in some cases powder X-ray diffraction analyses (*e.g.* Spence, 1988; Buseck *et al.*, 1988). More recently, there have been applications of conventional direct methods to decode data from TED information alone. While this has been shown to work in many cases (*e.g.* Dorset & Gilmore, 2000; Weirich *et al.*, 2000), it can also fail. The majority of this work has completely neglected any dynamical effects, which can, as shown by Sinkler & Marks (1999), lead to enhancement of the light atoms.

In a previous paper (Hu *et al.*, 2000, hereafter HCHM), we showed how in a 1*s* channeling model the partial success of direct methods can be understood *via* an 'effective kinematical approximation'; in a statistical sense, the phase distribution for the $\sum_0$ relationship shows a strong peak. Hence, even when kinematical theory is not valid in a strict numerical sense, it can still be a good approximation to the statistical phase distribution.

In this paper, we take the concept of combining dynamical diffraction theory and the statistical approach of direct methods one step further, to the $\sum_{2,0}$ triplet relationships [there is a total of eight distinct $\sum_2$ triplets, see *e.g.* Hauptman (1982)]. We will show both analytically and *via* numerical simulations that a straightforward complex extension works well.

2. Analysis

We will briefly repeat the statistical analysis for the $\sum_0$ invariant (derived in more detail in HCHM), aiming to introduce the necessary mathematical formalism. We can write a complete solution for the electron wavefunction in a thin crystal as a sum over 'two-dimensional' eigenstates $\Psi_n(\mathbf{R},z)$, where $\mathbf{R}=(x,y)$ is a two-dimensional vector perpendicular to the electron-beam direction z, namely:

$$\Psi(\mathbf{R},z)=1+\sum_n a_n\Psi_n(\mathbf{R})\{\exp[-i\pi(E_n/E_0)\kappa z]-1\}. \quad (1)$$

The sum in (1) is over the eigenstates labeled n, with occupations a_n. Each eigenstate has a characteristic oscillation frequency as a function of depth z, which is determined by the channeling (Bloch-wave) eigenvalue E_n (E_0 being the incident electron energy and $\kappa=\lambda^{-1}$). For a thin crystal, this series solution can be legitimately truncated after including only the most significant terms. For moderate values of sample thickness and atomic numbers, a further simplification of (1) can be used for cases in which the atomic columns are well separated in projection so that the atomic potentials do not strongly overlap (Van Dyck & Op de Beeck, 1996). In such cases, the lowest-lying eigenstates E_j (analogous to the jth atomic 1*s* states) mainly contribute to the sum on the right-hand side of (1), so the electron wavefunction may be written as

$$\Psi(\mathbf{R},z)=1+2i\sum_j a_j\Psi_j(\mathbf{R}-\mathbf{R}_j)\exp[-i\pi(E_j/2E_0)\kappa z]\times\sin[\pi(-E_j/2E_0)\kappa z], \quad (2)$$

where the sum is over the jth atomic positions.

In reciprocal space, which is used in structural crystallography, the normalized structure amplitude for the $\mathbf{g}$ reflection has the form

$$U_{\mathbf{g}}\equiv iF_{\mathbf{g}}=(i/\varepsilon_{\mathbf{g}}^{1/2})\sum_{j=1}^{N}|F_{j\mathbf{g}}|\exp[i(\delta_{j\mathbf{g}}-2\pi\mathbf{g}\cdot\mathbf{r}_j)], \quad (3)$$

where

$$F_{j\mathbf{g}} = |F_{j\mathbf{g}}| \exp(i\delta_{j\mathbf{g}}) \quad (4)$$

$$= 2V_j(\mathbf{g}) \exp[-i\pi(E_j/2E_0)\kappa z] \sin[\pi(-E_j/2E_0)\kappa z] \quad (5)$$

is the complex atomic column scattering amplitude of the atomic column labeled j, $\mathbf{r}_j$ is its position vector and N is the number of atomic columns in the two-dimensional unit cell. The normalization factor $\varepsilon_{\mathbf{g}}$ is equal to

$$\varepsilon_{\mathbf{g}} = \sum_{j=1}^{N} |F_{j\mathbf{g}}|^2 \quad (6)$$

and $V_j(\mathbf{g})$ is the Fourier transform of the jth atomic column wavefunction $\Psi_j(\mathbf{R} - \mathbf{R}_j)$, to a first approximation the kinematical single-atom structure factor. In the limit of a vanishingly small thickness, one has then $\psi(\mathbf{g}) = 0$ $[\varphi(-\mathbf{g}) = -\varphi(\mathbf{g})]$. The conditional probability distribution (CPD) $P(\psi(\mathbf{g})|R_{\mathbf{g}}, R_{-\mathbf{g}})$ defined for the value of $\psi(\mathbf{g})$ and the two magnitudes $R_{\mathbf{g}} = |U_{\mathbf{g}}|$, $R_{-\mathbf{g}} = |U_{-\mathbf{g}}|$ may be written as (Hauptman, 1982)

$$P(\psi(\mathbf{g})|R_{\mathbf{g}}, R_{-\mathbf{g}}) = \left[2\pi I_0\left(\frac{2R_{\mathbf{g}}R_{-\mathbf{g}}X}{1-X^2}\right)\right]^{-1} \exp\left\{\left(\frac{2R_{\mathbf{g}}R_{-\mathbf{g}}X}{1-X^2}\right) \times \cos[\psi(\mathbf{g}) + \xi(\mathbf{g})]\right\}. \quad (7)$$

Here the $\sum_0$ CPD parameters X and ξ are given by

$$X_{\mathbf{g}} \exp(-i\xi_{\mathbf{g}}) = (1/\varepsilon_{\mathbf{g}}) \sum_{j=1}^{N} |F_{j\mathbf{g}}|^2 \exp(2i\delta_{j\mathbf{g}}) \quad (8)$$

and I_0 is the modified Bessel function. It follows from (7) that the $\sum_0$ CPD has a single maximum at $\psi_{\mathbf{g}} = -\xi_{\mathbf{g}}$ (the $\sum_0$ invariant) and the two-phase structure variable is distributed around the value of $-\xi_{\mathbf{g}}$ with a width $\Delta\psi \approx A_{\mathbf{g}}^{-1/2}$. The latter is relatively narrow if the variance of the $\sum_0$ CPD is small, which is inversely proportional to

$$A_{\mathbf{g}} = R_{\mathbf{g}}R_{-\mathbf{g}}X_{\mathbf{g}}/(1 - X_{\mathbf{g}}^2). \quad (9)$$

If we go back to equation (3) and stay in the frame of 1s-state channeling, the phase of the complex atomic scattering amplitude δ_j does not depend on the diffraction vector $\mathbf{g}$, only on the thickness variable z. Hence, of particular importance, the subscript $\mathbf{g}$ can be omitted in the symbols $\delta_{j\mathbf{g}}$, $X_{\mathbf{g}}$ and $\xi_{\mathbf{g}}$,

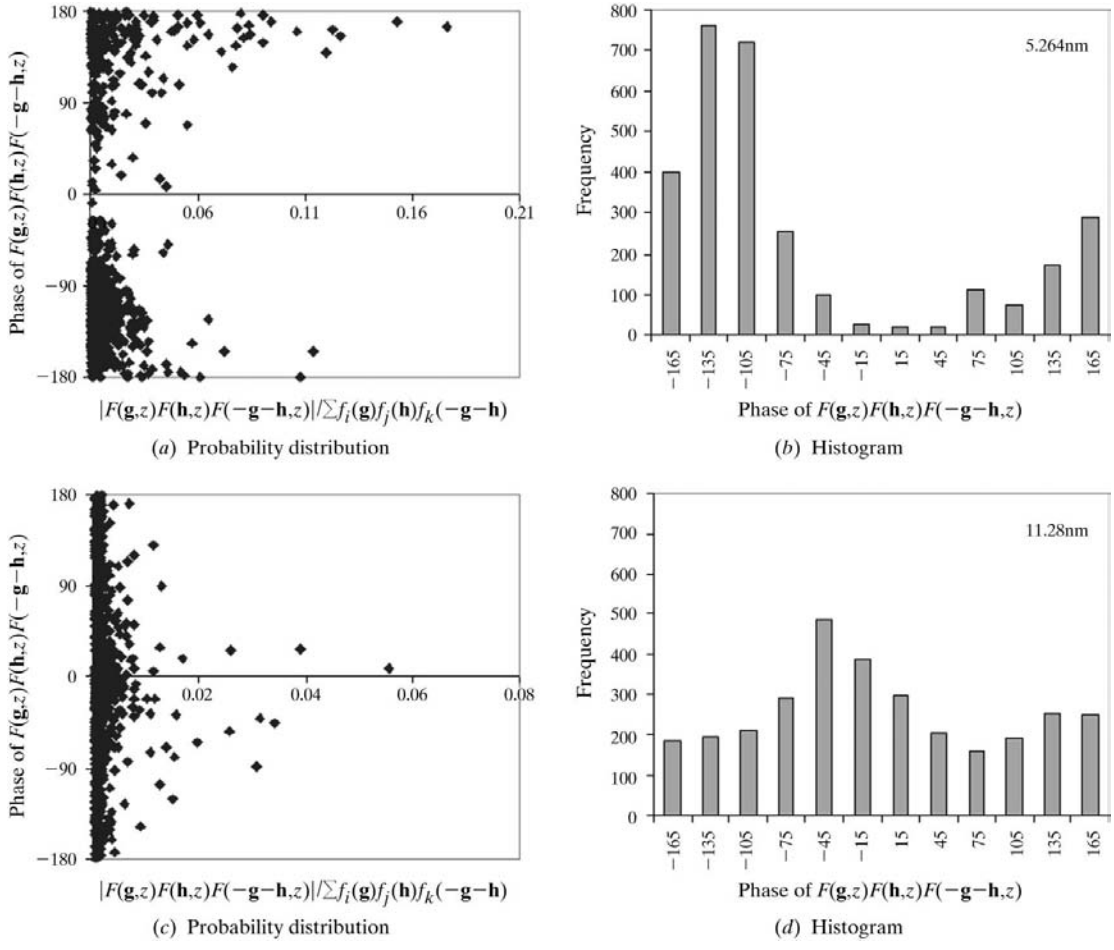

Figure 1
The probability distribution and histogram of the phases of the triple products of dynamical structure factors $F(\mathbf{g},z)F(\mathbf{h},z)F(-\mathbf{g}-\mathbf{h},z)$. The crystal thickness z along the [001] zone axis of $C_{32}Br_{16}CuN_8$ is: (*a*), (*b*) 5.264 nm; (*c*), (*d*) 11.28 nm. Note that a non-zero triple product cannot be accounted for with conventional direct methods, but can in principle be exploited in a modified algorithm as discussed later.

and the $\sum_0$ invariants (equal to $-\xi$) are independent of the diffraction vector **g** within a 1*s* channeling model. Particularly noteworthy here is that to a good approximation the $\sum_0$ invariant is unique and non-zero for a non-centrosymmetric structure where Friedel's law for $\pm\mathbf{g}$ reflection pairs does not hold.

2.1. The joint probability $\sum_2$ distribution

Hereafter, we will follow Hauptman's treatment of the probabilistic theory of three-phase structure invariants for the case of complex atomic scattering factors (Hauptman, 1982; see above for notations as well), making appropriate simplifications for the special case of a 1*s* channeling model for the dynamical electron diffraction (Van Dyck & Op de Beeck, 1996; Sinkler & Marks, 1999; Hu & Tanaka, 1999). Since many of the relevant equations for the variables have been previously given by Hauptman (1982) and are rather long, they will not be repeated here.

Let us assume that **g**, **h** and **k** are diffraction vectors satisfying the relationship

$$\mathbf{g}+\mathbf{h}+\mathbf{k}=0. \tag{10}$$

Owing to the breakdown of Friedel's law in the general case of dynamical diffraction, each of the eight $\sum_2$ invariants is defined in terms of the six magnitudes:

$$R_1=|U_{\mathbf{g}}|,\ R_{-1}=|U_{-\mathbf{g}}|;\ \ R_2=|U_{\mathbf{h}}|,\ R_{-2}=|U_{-\mathbf{h}}|;\\ R_3=|U_{\mathbf{k}}|,\ R_{-3}=|U_{-\mathbf{k}}|; \tag{11}$$

which are not in general equal in pairs, and where the normalized structure factors $U_{\pm\mathbf{g}}$ are defined by (3).

The joint probability distribution of the magnitudes R_j, R_{-j} and the phases φ_j, φ_{-j} of the structure factors $F_{\pm j}$ ($j=1,2,3$) is given by Hauptman's formula and takes the following form here:

$$\begin{aligned}P_2(&R_1,R_{-1},R_2,R_{-2},R_3,R_{-3};\varphi_1,\varphi_{-1},\varphi_2,\varphi_{-2},\varphi_3,\varphi_{-3})\\ &\cong \pi^{-6}R_1R_{-1}R_2R_{-2}R_3R_{-3}(1-X^2)^{-3}\\ &\times\exp[-(R_1^2+R_{-1}^2+R_2^2+R_{-2}^2+R_3^2+R_{-3}^2)/(1-X^2)]\\ &\times\exp\{2X[R_1R_{-1}\cos(\textstyle\sum_{0,1}+\xi)+R_2R_{-2}\cos(\sum_{0,2}+\xi)\\ &+R_3R_{-3}\cos(\textstyle\sum_{0,3}+\xi)]/(1-X^2)\}\exp\big(2(1-X^2)^{-3}\\ &\times\{Z_0[R_1R_2R_3\cos(\textstyle\sum_{2,0}-\zeta_0)+R_{-1}R_{-2}R_{-3}\\ &\times\cos(\textstyle\sum_{2,-0}-\zeta_0)]+Z[R_{-1}R_2R_3\cos(\sum_{2,1}-\zeta)\\ &+R_1R_{-2}R_{-3}\cos(\textstyle\sum_{2,-1}-\zeta)]+Z[R_1R_{-2}R_3\cos(\sum_{2,2}-\zeta)\\ &+R_{-1}R_2R_{-3}\cos(\textstyle\sum_{2,-2}-\zeta)]+Z[R_1R_2R_{-3}\cos(\sum_{2,3}-\zeta)\\ &+R_{-1}R_{-2}R_3\cos(\textstyle\sum_{2,-3}-\zeta)]\}\big).\end{aligned} \tag{12}$$

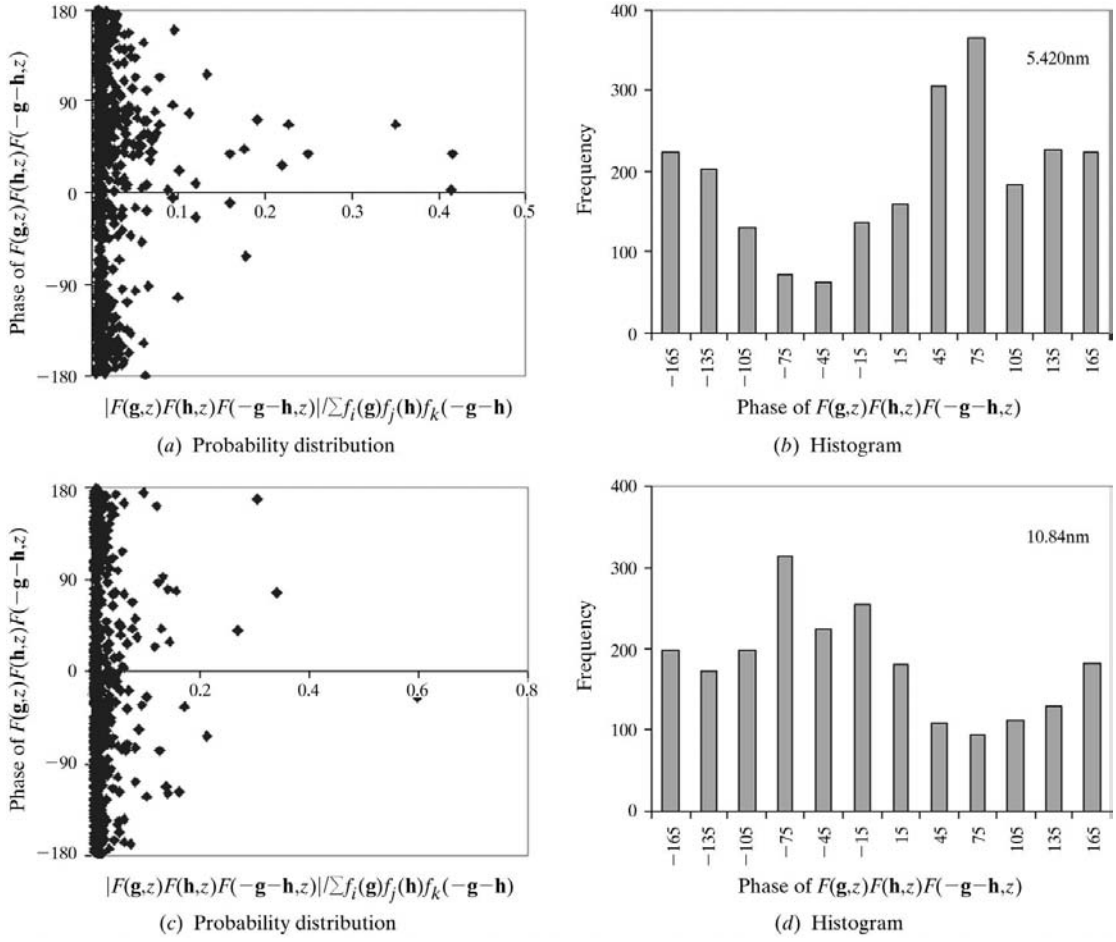

Figure 2
The probability distribution and histogram of the phases of the triple products of dynamical structure factors $F(\mathbf{g},z)F(\mathbf{h},z)F(-\mathbf{g}-\mathbf{h},z)$. The crystal thickness z along the [001] zone axis of $YSr_2Cu_2GaO_7$ is: (*a*), (*b*) 5.42 nm; (*c*), (*d*) 10.84 nm.

The parameters Z, ζ are uniquely defined by the equation

$$Z\exp(i\zeta) = \gamma + i\sigma, \tag{13}$$

where the parameters γ, σ are given by Hauptman (1982), keeping in mind that here

$$\gamma_1 = \gamma_2 = \gamma_3 = \gamma,\ \ \sigma_1 = \sigma_2 = \sigma_3 = \sigma, \tag{14}$$

so that

$$Z_1 = Z_2 = Z_3 = Z,\ \ \zeta_1 = \zeta_2 = \zeta_3 = \zeta \tag{15}$$

and

$$\begin{aligned}\gamma &= C_{1,2,3}[-C + (C^2 - S^2)] + S_{1,2,3}[-S + 2CS] \\ &\quad + C_{-1,2,3}[1 - 2C + 2(C^2 + S^2) - (C^3 + CS^2)] \\ &\quad + S_{-1,2,3}[-2S - (S^3 + C^2S)], \\ \sigma &= C_{1,2,3}[S + 2CS] + S_{1,2,3}[-C - (C^2 - S^2)] \\ &\quad + C_{-1,2,3}[-2S - (S^3 + C^2S)] \\ &\quad + S_{-1,2,3}[1 + 2C + 2(C^2 + S^2) + (C^3 + CS^2)].\end{aligned}$$

Here the coefficients C and S, $C_{1,2,3}$ and $S_{1,2,3}$, $C_{-1,2,3}$ and $S_{-1,2,3}$ are defined as [*cf.* equations (4), (6), (8)]

$$\begin{aligned}C + S &\equiv X\exp(i\zeta), \\ C_{1,2,3} &= (\varepsilon_{\mathbf{g}}\varepsilon_{\mathbf{h}}\varepsilon_{\mathbf{k}})^{-1/2}\sum_{j=1}^{N}|F_{j\mathbf{g}}F_{j\mathbf{h}}F_{j\mathbf{k}}|\cos(3\delta_j), \\ S_{1,2,3} &= (\varepsilon_{\mathbf{g}}\varepsilon_{\mathbf{h}}\varepsilon_{\mathbf{k}})^{-1/2}\sum_{j=1}^{N}|F_{j\mathbf{g}}F_{j\mathbf{h}}F_{j\mathbf{k}}|\sin(3\delta_j), \\ C_{-1,2,3} &= (\varepsilon_{\mathbf{g}}\varepsilon_{\mathbf{h}}\varepsilon_{\mathbf{k}})^{-1/2}\sum_{j=1}^{N}|F_{j\mathbf{g}}F_{j\mathbf{h}}F_{j\mathbf{k}}|\cos(2\delta_j), \\ S_{-1,2,3} &= (\varepsilon_{\mathbf{g}}\varepsilon_{\mathbf{h}}\varepsilon_{\mathbf{k}})^{-1/2}\sum_{j=1}^{N}|F_{j\mathbf{g}}F_{j\mathbf{h}}F_{j\mathbf{k}}|\sin(2\delta_j).\end{aligned}$$

The following notations for the $\sum_{0,j}$ pairs ($j = 1, 2, 3$) and the $\sum_{2,\pm j}$ triplets ($j = 0, 1, 2, 3$) are used in (12):

$$\sum\nolimits_{0,j} = \varphi_j + \varphi_{-j}, \tag{16}$$

$$\begin{aligned}\sum\nolimits_{2,j} &= \varphi_1 + \varphi_2 + \varphi_3 - 0.5j(j-2)(j-3)\sum\nolimits_{0,1} \\ &\quad + 0.5j(j-1)(j-3)\sum\nolimits_{0,2} - (1/6)j(j-1)(j-2)\sum\nolimits_{0,3},\end{aligned} \tag{17}$$

$$\begin{aligned}\sum\nolimits_{2,-j} &= \varphi_{-1} + \varphi_{-2} + \varphi_{-3} - 0.5j(j-2)(j-3)\sum\nolimits_{0,1} \\ &\quad + 0.5j(j-1)(j-3)\sum\nolimits_{0,2} - (1/6)j(j-1)(j-2)\sum\nolimits_{0,3}.\end{aligned} \tag{18}$$

2.2. The conditional probability $\sum_2$ distribution

The conditional probability distribution (CPD) of each of $\sum_{2,\pm j}$ assuming as known the six magnitudes (11) together with the weights $A_{\pm j}$ (see below) in terms of the complex normalized structure factors can be obtained from (12) by integrating the joint probability distribution with respect to three of the six $\varphi_{\pm j}$ ($j = 1, 2, 3$) except those yielding the $\sum_{2,\pm j}$ triplet. A direct integration for the $\sum_{2,\pm j}$ CPD (see Hauptman, 1982, for details) yields

$$P_j(\textstyle\sum_{2,\pm j}) = K_{\pm j}^{-1}\exp[2A_{\pm j}\cos(\sum_{2,\pm j} - \omega_{\pm j})]. \tag{19}$$

Here the parameters $A_{\pm j}$ and $\omega_{\pm j}$ are given by ($j = 0, 1, 2, 3$)

$$A_{\pm j} = 0.5B_{\pm j}(1 - X^2)^{-3}, \quad B_{\pm j}\exp(i\omega_{\pm j}) = C_{\pm j} + iS_{\pm j}, \tag{20}$$

with $K_{\pm j} = 2\pi I_0(2A_{\pm j})$, I_0 being the modified Bessel function and the coefficients $C_{\pm j}$, $S_{\pm j}$ are given by Hauptman (1982) subject to the additional conditions of (13).

We will confine our analysis to the $\sum_{2,\pm 0}$ triplets, the most important ones for a direct-methods analysis. The coefficients $C_{\pm 0}$, $S_{\pm 0}$ for each of the conditional probability distributions $P_0(\sum_{2,\pm 0})$ take the form

$$\begin{aligned}C_0 &= Z_0[R_1R_2R_3\cos(\zeta_0) + R_{-1}R_{-2}R_{-3}\tau_1\tau_2\tau_3\cos(3\xi + \zeta_0)] \\ &\quad + Z[R_{-1}R_2R_3\tau_1\cos(\xi - \zeta) + R_1R_{-2}R_{-3}\tau_2\tau_3\cos(2\xi + \zeta)] \\ &\quad + Z[R_1R_{-2}R_3\tau_2\cos(\xi - \zeta) + R_{-1}R_2R_{-3}\tau_1\tau_3\cos(2\xi + \zeta)] \\ &\quad + Z[R_1R_2R_{-3}\tau_3\cos(\xi - \zeta) + R_{-1}R_{-2}R_3\tau_1\tau_2\cos(2\xi + \zeta)],\end{aligned} \tag{21a}$$

$$\begin{aligned}S_0 &= Z_0[R_1R_2R_3\sin(\zeta_0) - R_{-1}R_{-2}R_{-3}\tau_1\tau_2\tau_3\sin(3\xi + \zeta_0)] \\ &\quad - Z[R_{-1}R_2R_3\tau_1\sin(\xi - \zeta) + R_1R_{-2}R_{-3}\tau_2\tau_3\sin(2\xi + \zeta)] \\ &\quad - Z[R_1R_{-2}R_3\tau_2\sin(\xi - \zeta) + R_{-1}R_2R_{-3}\tau_1\tau_3\sin(2\xi + \zeta)] \\ &\quad - Z[R_1R_2R_{-3}\tau_3\sin(\xi - \zeta) + R_{-1}R_{-2}R_3\tau_1\tau_2\sin(2\xi + \zeta)],\end{aligned} \tag{21b}$$

$$\begin{aligned}C_{-0} &= Z_0[R_{-1}R_{-2}R_{-3}\cos(\zeta_0) + R_1R_2R_3\tau_1\tau_2\tau_3\cos(3\xi + \zeta_0)] \\ &\quad + Z[R_1R_{-2}R_{-3}\tau_1\cos(\xi - \zeta) + R_{-1}R_2R_3\tau_2\tau_3\cos(2\xi + \zeta)] \\ &\quad + Z[R_{-1}R_2R_{-3}\tau_2\cos(\xi - \zeta) \\ &\quad + R_1R_{-2}R_{-3}\tau_1\tau_3\cos(2\xi + \zeta)] \\ &\quad + Z[R_{-1}R_{-2}R_3\tau_3\cos(\xi - \zeta) \\ &\quad + R_1R_2R_{-3}\tau_1\tau_2\cos(2\xi + \zeta)],\end{aligned} \tag{22a}$$

$$\begin{aligned}S_{-0} &= Z_0[R_{-1}R_{-2}R_{-3}\sin(\zeta_0) - R_1R_2R_3\tau_1\tau_2\tau_3\sin(3\xi + \zeta_0)] \\ &\quad - Z[R_1R_{-2}R_{-3}\tau_1\sin(\xi - \zeta) + R_{-1}R_2R_3\tau_2\tau_3\sin(2\xi + \zeta)] \\ &\quad - Z[R_{-1}R_2R_{-3}\tau_2\sin(\xi - \zeta) + R_1R_{-2}R_3\tau_1\tau_3\sin(2\xi + \zeta)] \\ &\quad - Z[R_{-1}R_{-2}R_3\tau_3\sin(\xi - \zeta) + R_1R_2R_{-3}\tau_1\tau_2\sin(2\xi + \zeta)],\end{aligned} \tag{22b}$$

and the positive parameters τ_j ($j = 1, 2, 3$) are given by

$$\tau_j = I_1(2A_j)/I_0(2A_j), \tag{23}$$

where I_1 and I_0 are modified Bessel functions, and the coefficient A_j is defined in (9).

There is an important simplification for a centrosymmetric crystal when the positive magnitudes of $R_{\pm j}$ and the phases $\varphi_{\pm j}$ are equal in pairs, when the two $\sum_{2,\pm 0}$ CPD merge into one unique distribution:

$$P_0^{(cs)}(\textstyle\sum_{2,0}) = K_0^{-1}\exp[2A_0\cos(\sum_{2,0} - \omega_0)], \tag{24}$$

with simplified forms for the two parameters (putting $R_j = R_{-j}$ in all the above formulae)

$$C_0/R_1R_2R_3 = Z_0[\cos(\zeta_0) + \tau_1\tau_2\tau_3\cos(3\xi+\zeta_0)] + Z[\tau_1\cos(\xi-\zeta) + \tau_2\tau_3\cos(2\xi+\zeta)] + Z[\tau_2\cos(\xi-\zeta) + \tau_1\tau_3\cos(2\xi+\zeta)] + Z[\tau_3\cos(\xi-\zeta) + \tau_1\tau_2\cos(2\xi+\zeta)], \quad (25a)$$

$$S_0/R_1R_2R_3 = Z_0[\sin(\zeta_0) - \tau_1\tau_2\tau_3\sin(3\xi+\zeta_0)] - Z[\tau_1\sin(\xi-\zeta) + \tau_2\tau_3\sin(2\xi+\zeta)] - Z[\tau_2\sin(\xi-\zeta) + \tau_1\tau_3\sin(2\xi+\zeta)] - Z[\tau_3\sin(\xi-\zeta) + \tau_1\tau_2\sin(2\xi+\zeta)]. \quad (25b)$$

To satisfy (24) in a strict sense requires that Friedel's law holds. However, even if there is a small deviation from Friedel's law in a statistical sense, the statistical distribution based on (24) may hold relatively well, a fact that will become apparent when we turn to numerical calculations (see below).

One further important simplification is possible. If the variance of the $\sum_{0,j}$ CPD proportional to A_j^{-1} ($j = 1, 2, 3$) is small, the parameters $\tau_1 \approx \tau_2 \approx \tau_3$ tend to unity asymptotically, see (23), so that

$$C_0/R_1R_2R_3 \approx Z_0[\cos(\zeta_0) + \cos(3\xi+\zeta_0)] + 3Z[\cos(\xi-\zeta) + \cos(2\xi+\zeta)], \quad (26a)$$

$$S_0/R_1R_2R_3 \approx Z_0[\sin(\zeta_0) - \sin(3\xi+\zeta_0)] - 3Z[\sin(\xi-\zeta) + \sin(2\xi+\zeta)]. \quad (26b)$$

Correspondingly, the expected mean phase $\sum_{2,0}$ value (the ω_0 invariant) is given by [see equations (20), (26)]

$$\omega_0 \approx \tan^{-1}\big(\{Z_0[\sin(\zeta_0) - \sin(3\xi+\zeta_0)] - 3Z[\sin(\xi-\zeta) + \sin(2\xi+\zeta)]\} \times \{Z_0[\cos(\zeta_0) + \cos(3\xi+\zeta_0)] + 3Z[\cos(\xi-\zeta) + \cos(2\xi+\zeta)]\}^{-1}\big). \quad (27)$$

Note that in the pure kinematical approximation when the phases $\delta_{j\mathbf{g}}$ of the jth atomic scattering factors (4) can be set to zero all the values ξ, ζ_0 and ζ_0 are zero, as is the ω_0 invariant. In the case in question, the expression (27) for the ω_0 invariant is rather complicated to estimate [see Hauptman (1982) and equations (13)–(15), (20), (26), (27)]. Fortunately, as pointed out by Hauptman (1982), an assessment of the ω_0 invariant is better if the variance of the distribution (24) is small, in other words, when the 'A_0 value' tends to be large. Specifically, this is

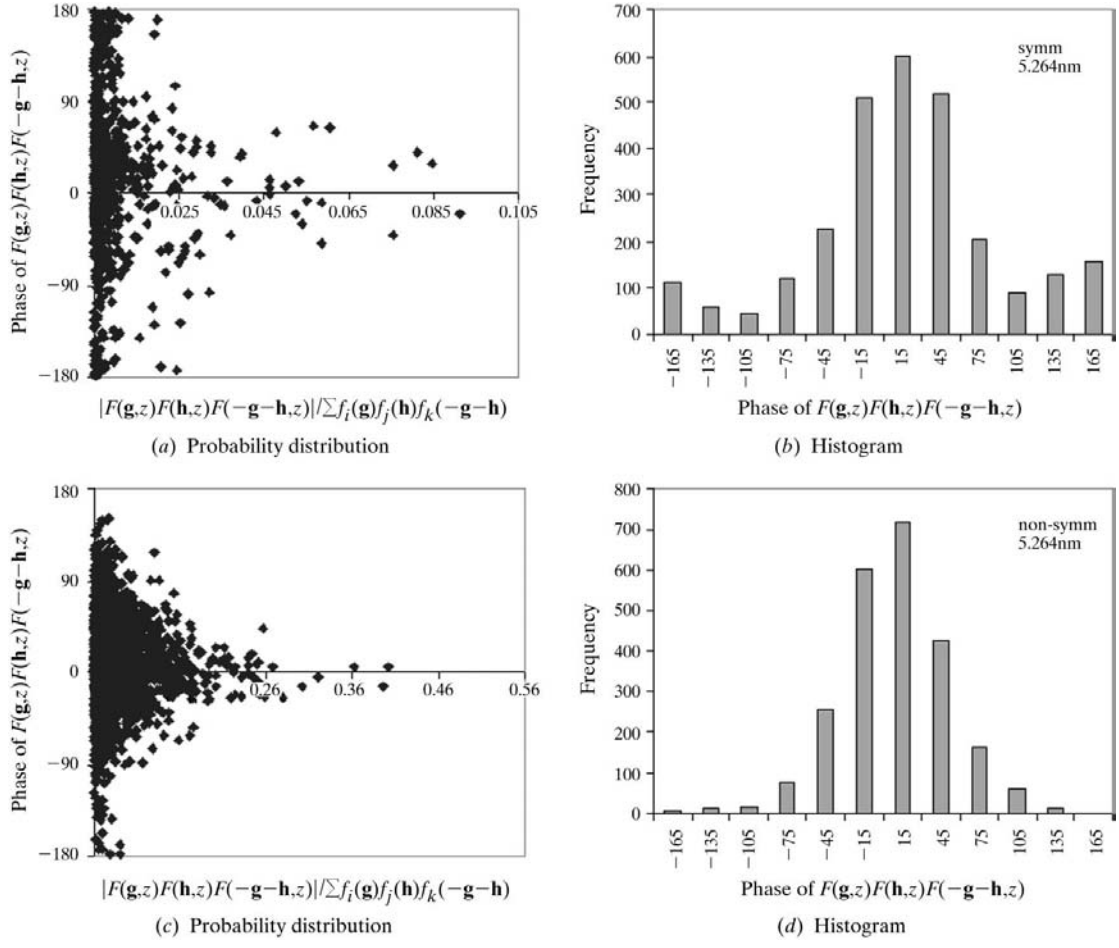

Figure 3
The probability distribution and histogram of the triple product $F(\mathbf{g},z)F(\mathbf{h},z)F(-\mathbf{g}-\mathbf{h},z)$ for the centrosymmetric and non-centrosymmetric (random) models of $C_{32}Cl_{16}CuN_8$. The sample thickness z along the [001] zone axis is 5.264 nm.

valid for the statistics based on the so-called strong triplets, one term of which may be the zero reflection. This gives a simple estimate for the ω_0 invariant, namely:

$$\omega_0 \cong \varphi(\mathbf{g}=\mathbf{0}) - \xi \ (\mathrm{mod}\, 2\pi), \tag{28}$$

where $\varphi(\mathbf{g}=\mathbf{0})$ is the phase of zero-reflection structure factor $F(\mathbf{g}=\mathbf{0})$ and $-\xi$ is Hauptman's invariant for the $\sum_0$ pairs. Note that using the so-called normalized phase values of the complex structure factors (see below) implies that

$$-\xi = \varphi(\mathbf{g}) + \varphi(-\mathbf{g}) \approx \varphi(\mathbf{g}) + \varphi(-\mathbf{h}) + \varphi(-\mathbf{g}-\mathbf{h}) = \omega_0 \neq 0, \tag{29}$$

a result very different from that of kinematical diffraction where $-\xi = \omega_0 = 0$.

Switching to the electron diffraction structure amplitudes $U_{\mathbf{g}}$ defined by (3), which will be used to build the phase probability plots from multislice calculations (see §3), the ω_0 invariant should be rewritten as

$$\Omega_0 = \Im[\ln U(\mathbf{g}=0)] + \Xi. \tag{30}$$

(Here we are introducing the Ξ invariant and the Ω_0 invariant for the $\sum_0$ pairs and the $\sum_{2,0}$ triplets extracted from calculated electron diffraction data, simply shifting $\Omega_0 = \omega_0 + 3/2\pi$ and $\Xi = -\xi + \pi$.) This redefinition is appropriate because the structure amplitudes used in the initial definition [equation (3)] contain an additional phase factor of $\pi/2$ that is absent in X-ray diffraction.

If the variance of the $\sum_{2,0}$ CPD proportional to A_0^{-1} is small for diffraction vectors **g**, **h**, **k** forming the triplet (10), the three-phase $\sum_{2,0}$ invariant is sharply distributed around a unique value Ω_0 directly linked *via* (29) with the phase of the zero-beam structure factor and the phase pair invariant Ξ. Furthermore, if the calculated electron diffraction structure amplitudes are 'normalized' using the value of the zero reflection structure factor, $\Im[\ln U(\mathbf{g}) - \ln U(\mathbf{g}=0)]$, the values of the invariants for the $\sum_{2,0}$ triplets and the $\sum_0$ pairs should be equal to each other for the simple statistical model discussed above, *i.e.*

$$\Omega_0 \cong \Xi. \tag{31}$$

Note that the above assertion will also be true for a non-centrosymmetric structure provided the deviation from Friedel's law is relatively small in a statistical sense, *i.e.* small for the stronger reflections. In short, from the theoretical point

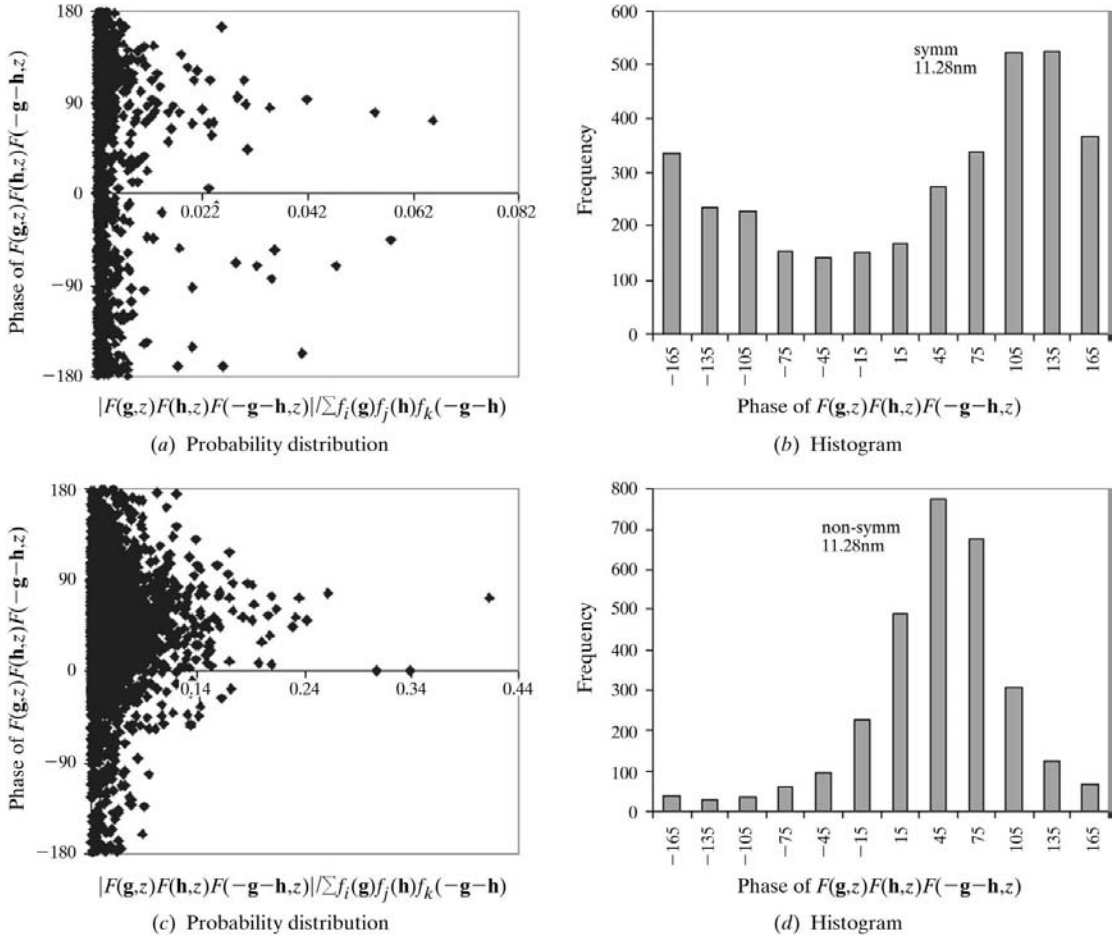

Figure 4
The probability distribution and histogram of the triple product $F(\mathbf{g},\mathbf{z})F(\mathbf{h},z)F(-\mathbf{g}-\mathbf{h},z)$ for the centrosymmetric and non-centrosymmetric (random) models of $C_{32}Cl_{16}CuN_8$. The sample thickness z along the [001] zone axis is 11.28 nm.

Table 1
Phase positions of the evaluated two- and three-phase structure invariants, Ξ (see HCHM for details) and Ω_0 (present work) for $C_{32}Br_{16}CuN_8$ (Fig. 1), $YSr_2Cu_2GaO_7$ (Fig. 2), $C_{32}Cl_{16}CuN_8$ (Figs. 3, 4, 6).

Present work	HCHM	Ξ (°)	Ω_0 (°)
Fig. 1(*b*)	Fig. 1(*d*)	−180	−135
Fig. 1(*d*)	Fig. 3(*d*)	15	−45
Fig. 2(*b*)	Fig. 4(*d*)	45	75
Fig. 2(*d*)	Fig. 5(*d*)	−180	−75
Fig. 3(*b*)	Fig. 7(*c*)	15	15
Fig. 3(*d*)	Fig. 7(*d*)	15	15
Fig. 4(*b*)	Fig. 8(*c*)	105	105
Fig. 4(*d*)	Fig. 8(*d*)	45	45
Fig. 6(*d*)	Fig. 9(*d*)	15	15
Fig. 6(*e*)	Fig. 9(*e*)	45	45
Fig. 6(*f*)	Fig. 9(*f*)	45	105

of view, the situation in question with the phase $\sum_{2,0}$ triplet looks similar to the analysis given previously in HCHM for the $\sum_0$ pairs. Inclusion of dynamical effects to a first approximation leads only to a shift away from zero of the two- and three-phase invariants, with the normalized values of Ξ and Ω_0 equal.

3. Results: numerical statistics tests

Using the known structure for perbromophthalocyanine $C_{12}Br_{16}CuN_8$, chlorinated copper phthalocyanine $C_{12}Cl_{16}CuN_8$ (see *e.g.* Dorset, 1995) and the superconducting ceramic $YSr_2Cu_2GaO_7$, the dynamic structure amplitudes $F(\mathbf{g},z)$ were calculated by the multislice method (see HCHM for details of the calculations), and the three-phase structure triplets equal to $\Im[\ln F(\mathbf{g},z)F(\mathbf{h},z)F(-\mathbf{g}-\mathbf{h},z)]$ were generated. Figs. 1 and 2 show numerically simulated three-phase probability distributions as a function of the magnitude of the unitary triplet

$$\left|F(\mathbf{g},z)F(\mathbf{h},z)F(-\mathbf{g}-\mathbf{h},z)\Big/\sum_{ijk} f_i(\mathbf{g})f_j(\mathbf{h})f_k(-\mathbf{g}-\mathbf{h})\right|$$

[$f_i(\mathbf{g})$ is the atomic scattering amplitude of the ith atom in a unit cell, the 0-beam triplet magnitude being normalized to 1] and histograms of the triplet-phase frequency for $C_{12}Br_{16}CuN_8$ at thicknesses of 5.264 and 11.28 nm, and for $YSr_2Cu_2GaO_7$ at thicknesses of 5.42 and 10.84 nm. As predicted by the analysis above, the CPD (15) shows relatively well structured maxima and minima separated by about 180°, whose widths increase as the thickness increases owing to reduction in the number of large amplitudes. Note that a non-zero triple product cannot be accounted for with conventional direct methods, but can in principle be exploited in a modified algorithm as discussed later.

The multislice-extracted results for the three-phase probability distributions and histograms of the triplet-phase frequency for the centrosymmetric structure of $C_{12}Cl_{16}CuN_8$ and a non-centrosymmetric ('random' model) modification of it are shown in Figs. 3 and 4 for sample thicknesses of 5.264 nm (Fig. 3) and 11.28 nm (Fig. 4). Again, we see that the $\sum_{2,0}$ CPD behavior occurs for a centrosymmetric structure. Remarkably, the non-centrosymmetric structure also obeys very well the $\sum_{2,0}$ CPD. According to the work of Hauptman (1982), the individual triple-phase invariants ω_0 and ω_{-0} should be different from each other and the statistical three-phase distribution for the different $\omega_{\pm 0}$ invariants have an unpredictable 'random' shape. However, in reality, the relationships $R_1 = R_{-1}$, $R_2 = R_{-2}$, $R_3 = R_{-3}$ hold in an average or 'statistical sense' (see Fig. 5), so the problem simplifies as suggested earlier in §2.2.

Finally, Fig. 6 shows simulated results for the centrosymmetric structure of $C_{12}Cl_{16}CuN_8$ at voltages of 100, 500 and 1000 kV and a sample thickness of 5.264 nm. These confirm the assertion made in our preceding paper that neither the statistical three-phase probability distributions nor the three-

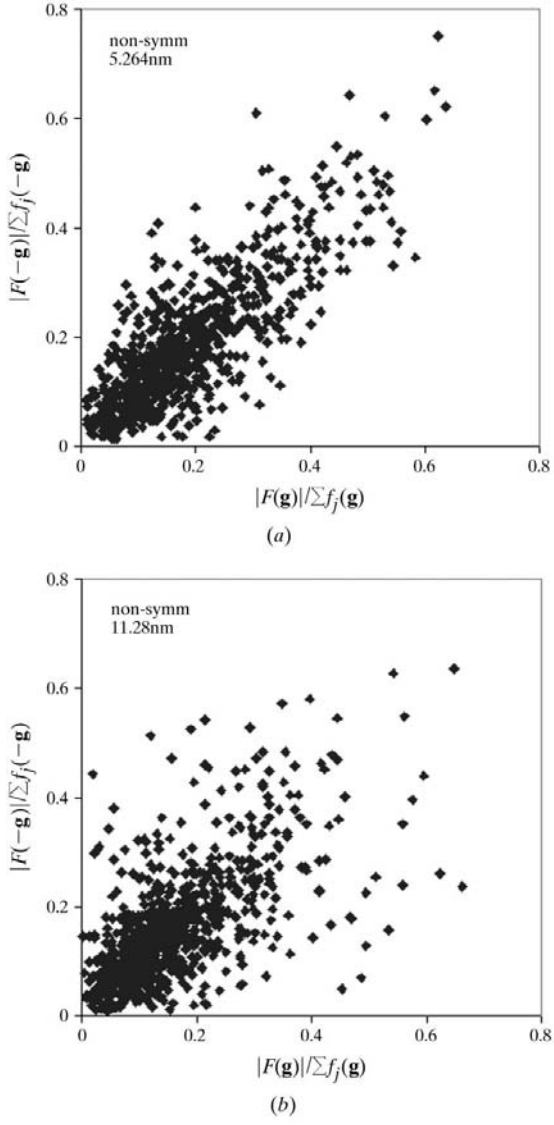

Figure 5
The numerically calculated plot of R_j *vs* R_{-j} corresponding to the random model of $C_{32}Cl_{16}CuN_8$ for the sample thicknesses: (*a*) 5.264 nm, (*b*) 11.28 nm.

phase frequency histograms are improved at higher voltage since electron diffraction does not simply tend towards a kinematical limit as the voltage is increased.

The corresponding evaluated values of the Ω_0 and the Ξ invariant for the statistical plots in Figs. 1–6 are listed in Table 1. It is worth emphasizing that except for $YSr_2Cu_2GaO_7$, for which a relatively large difference in the positions of the Ω_0 and Ξ invariant is observed owing to the reduction in the number of large amplitudes, the statistical distribution of the phase $\sum_{2,0}$ triplets holds in all the calculated examples.

4. Conclusions

Let us repeat the main points of our analysis, a statistical approach for dynamical electron diffraction structure amplitudes:

(i) We describe the dynamical electron diffraction using a simple channeling approximation (see *e.g.* Van Dyck & Op de Beeck, 1996) coupled with Hauptman's probabilistic theory and techniques (Hauptman, 1982) for direct methods with anomalous dispersion.

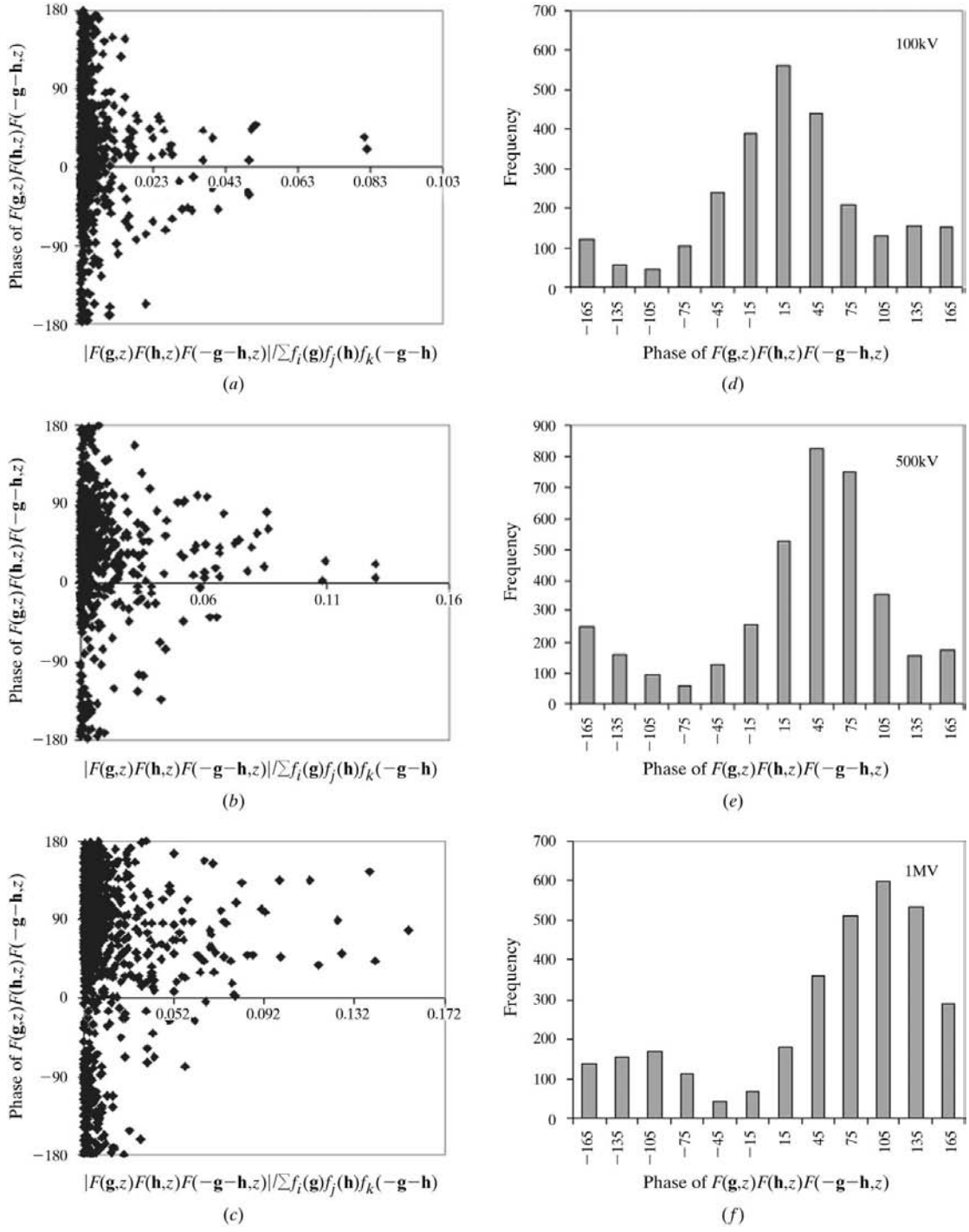

Figure 6
The probability three-phase distribution and histogram of $C_{32}Cl_{16}CuN_8$ for different values of accelerating voltage: (*a*), (*d*) 100 kV; (*b*), (*e*) 500 kV; (*c*), (*f*) 1 MV. The sample thickness z along the [001] zone axis is 5.264 nm.

(ii) The basic 1*s* channeling approach that is valid for relatively thin samples simplifies the complex electron structure amplitudes in such a way that the mean average values of the CPD of the two- and three-phase complex structure amplitudes, the Ξ invariant and Ω_0 invariant, do not depend on the diffraction vectors involved.

(iii) If both the above assumptions hold, the unique CPDs of the two- and three-phase complex structure amplitudes can be determined (§2). The simplified statistical model developed yields that the normalized (by the phase of the zero structure amplitude) values of the Ξ invariant and Ω_0 invariant are equal to each other.

(iv) The theoretical model is applied to analysis of numerically simulated statistics of the two- (HCHM, 2000) and the three-phase structure-amplitude distributions obtained from rigorous numerical solutions of Shrödinger's equation for different structures. Note that the Ξ-invariant and Ω_0-invariant values are in general unknown unless the structure is known, unlike direct methods with anomalous dispersion where the values of the complex atomic structure factors are known *a priori* (*cf*. Hauptman, 1982).

The numerical results presented in the previous section are in qualitative agreement with the distribution analysis of §2. While it is certainly not true or even close to true to state that the diffraction is kinematical, in a statistical sense the $\sum_{2,0}$ CPD is relatively narrow for some realistic sample thickness, similar to the $\sum_0$ CPD analyzed previously. To condense this into very simple mathematical terms, from equations (29) and (30) we can apply a phase shift of $0.4\Xi(z)$ to minimize the absolute values of $\sum_0$ and $\sum_{2,0}$ invariants. The phase-shifted normalized structure factors can be relatively well approximated as

$$U'_g(z) \approx \varphi(\mathbf{g}, z)\exp[i0.4\Xi(z)] \qquad (32)$$

if and only if $\Omega_0(z)$ and $\Xi(z)$ are small with a phase error of about $0.2\Omega_0(z)$, provided that Friedel's law holds and/or its breakdown is insignificant, where $\varphi(\mathbf{g},z)$ is the Fourier transform of a real function which we call the effective potential and $\Xi(z)$ the thickness-dependent $\sum_0$ invariant, and the approximation is better obeyed for the stronger reflections in reciprocal space. Note that in general neither $\Omega_0(z)$ nor $\Xi(z)$ can be directly measured experimentally (except *via* holography), and they cannot be calculated ahead of time. If one enforces that the $\sum_0$ CPD value $\Xi = 0$, the phase errors from dynamical effects will be of order $\Omega_0(z)/3$, which may be tolerable. Conventional direct methods applied to the diffraction data will tend to recover this effective potential, which may (but does not have to) show the heavier atoms. We have the rather remarkable result that conventional direct methods will work to a certain extent in the complete neglect of dynamical effects and with simple kinematical $\sum_{2,0}$ relationships in a *statistical* sense. Of course this does not mean that the structure can be refined without including dynamical effects and it would be a pure fluke if it could be. However, an approximate structure is often more than good enough to solve real problems. In general, a better approach would be to take $\Omega_0(z)$ and $\Xi(z)$ as reciprocal-lattice-vector-independent constants whose values can be permuted along with the phases of the normalized structure amplitudes.

A few final comments are appropriate here about what will happen with thicker samples and orientations that do not project so well into atomic columns. As is evident from the calculated data, as the crystal thickness increases there is a tendency for the absolute value of the (normalized) dynamical structure factors to decrease. Since dynamical diffraction generally shows an oscillatory character with sample thickness, there may be thicker regions where large structure factors exist (and direct methods will work) but not as well as for thin samples. For samples that do not project so well into atomic columns, so the 1*s* channeling reduction is less valid, to a first approximation the diffraction will be less dynamical so deviations from kinematical and conventional direct-methods approaches should not be so severe. Unfortunately, this implies that it is probably incorrect to merge data from a number of different zones to form a composite data set on which to use three-dimensional direct methods. How to solve the later problem, as well as how to invert from the effective dynamical potential to atomic sites automatically remain topics for future research.

This work was supported by the Science and Technology Center for Superconductivity on NSF-grant number DMR 91-20000 and seed funding from the Center for Catalysis and Surface Science at Northwestern University.

References

Buseck, P. R., Cowley, J. M. & Eyring, L. (1988). Editors. *High-Resolution Transmission Electron Microscopy and Associated Techniques*. Oxford University Press.
Dorset, D. L. (1995). *Structural Electron Crystallography*, pp. 188–202. New York/London: Plenum Press.
Dorset, D. L. & Gilmore, C. J. (2000). *Acta Cryst.* A**56**, 62–67.
Hauptman, H. (1982). *Acta Cryst.* A**38**, 632–641.
Hu, J. J., Chukhovskii, F. N. & Marks, L. D. (2000). *Acta Cryst.* A**56**, 458–469.
Hu, J. J. & Tanaka, N. (1999). *Ultramicroscopy*, **80**, 1–5.
Sinkler, W. & Marks, L. D. (1999). *Ultramicroscopy*, **75**, 251–268.
Spence, J. C. H. (1988). *Experimental High-Resolution Electron Microscopy*. Oxford University Press.
Van Dyck, D. & Op de Beeck, M. (1996). *Ultramicroscopy*, **64**, 99–107.
Weirich, T. E., Zou, X., Ramlau, R., Simon, A., Cascarano, G. L., Giocovazzo, C. & Hovmöller, S. (2000). *Acta Cryst.* A**56**, 29–35.